J Mater Sci (2008) 43:1241–1248
DOI 10.1007/s10853-007-2272-8

Influence of torsion deformation on microstructure of cold-drawn pearlitic steel wire

Catherine Cordier-Robert · Benoît Forfert · Bernard Bolle · Jean-Jacques Fundenberger · Albert Tidu

Received: 20 April 2007 / Accepted: 29 October 2007 / Published online: 4 December 2007

Abstract A comparative microstructural analyse of cold-drawn pearlitic steel wires in as-drawn and after an additional torsion deformation states is presented in this paper. During torsion the temperature of the wire increases to attain 90 °C. Then the microstructure of wires is the result of different events effects, as initial drawing, temperature increase and torsion deformation. Individually or in association, both events influence the stress level and nature in ferrite and cementite lamellae, modify the kinetic of cementite decomposition and change the dislocation mobility in cementite and ferrite. Carbon atoms migration from cementite to ferrite is affected by these thermomechanical treatments inducing a modification of dislocation pinning by carbon atoms and lamellae interfaces. The phases' determination and quantification, associated with the carbon content variation in each phase was investigated by Mössbauer spectroscopy. The evolution of the pearlitic steel wires microstructure will be discussed point-by-point, as a function of applied deformation nature.

C. Cordier-Robert
Laboratoire de Métallurgie Physique et Génie des Matériaux (LMPGM), UMR CNRS 8517, Université des Sciences et Technologies de Lille, Cité Scientifique, Villeneuve d'Ascq Cedex 59655, France

B. Forfert · B. Bolle · J.-J. Fundenberger
Laboratoire d'Etude des Textures et Application aux Matériaux (LETAM), UMR CNRS 7078, Université Paul Verlaine de Metz, Ile du Saulcy, Metz Cedex 01 57045, France

A. Tidu (✉)
Laboratoire d'Etude des Textures et Application aux Matériaux (LETAM), UMR CNRS 7078, Ecole Nationale d'Ingénieurs de Metz, Ile du Saulcy, Metz Cedex 01 57045, France
e-mail: tidu.albert@univ-metz.fr

Introduction

Drawn pearlitic steels wires are widely used in automotive industry, engineering bridges building for theirs unusual strain-hardening behaviour, as well as for the high strength with acceptable level of ductility.

The large amount of potential applications of drawn wires induce that, the last 10 years, lot of authors have studied mechanical properties and microstructure of drawn pearlitic steel wires. Mechanical investigations were performed by ductility or hardness measurements and thermomagnetic studies in using highly sensitive differential magnetometer [1]. Microstructural observations were obtained by transmission electron microscopy (TEM), atom probe field ion microscopy (APFIM), three dimensional atom probe (3DAP), internal friction [2] and Mössbauer spectroscopy [1]. It has been revealed that the drawing of pearlitic steel wires leads to a microstructure evolution associated to mechanical properties modifications [3]. The local increase of carbon content in lamellar ferrite is shown to be the main reason for loss of steel ductility [3]. The hardening of the drawn pearlitic steels is observed when the lamellar spacing of pearlite is decreasing and the dislocation density is increasing [3].

The typical chemical composition of pearlitic steels wires is nearly eutectoid and the microstructure is consisting of ferrite and cementite. Prior drawing deformation, eutectoid steels microstructure is constituted of fine lamellar ferrite and lamellar cementite. In cold-drawn pearlitic steel wires, the initial interlamellar spacing was due to the low transformation temperature [4]. Successive drawing passes are responsible of increasing strain by severe plastic deformation, pearlite lamellar spacing decrease [5, 6], cementite decomposition [2, 4], dissolution of cementite plates in lamellae into ferrite matrix [6], and a

local increased of carbon concentration in lamellar ferrite [4, 7]. The dissolution of cementite in association with an increasing of the carbon content in ferrite, at room temperature, during the drawing process, are interesting phenomena because at this temperature cementite is supposed to be thermodynamically stable and the carbon solubility in ferrite small.

Studies of drawn steel wires were devoted to measurements, by neutron diffraction technique, of texture and residual stress states in ferrite and cementite phases and to stress nature characterisation [8–10]. In the same time, other authors proposed some modelling of stress and texture [11–13].

Both studies demonstrate a change of lamellae spacing with the level of tensile plastic deformation and with the pearlitic or ferritic steel nature [8]. So, lamellae spacing increases with increasing of tensile stress close to the tensile strength and then decreases up to be equal to the initial value [8]. Lamellar ferrite–cementite structure was found to hold residual thermal stress caused by different thermal expansion coefficient. The level of residual thermal stress depends on the stress relaxation ability [9]. The drawing mechanical treatment induces a plastic anisotropy and stresses develop inside individual bcc crystallites [12]. Yu et al. proposed a model allowing estimation of the macrostresses acting on the scale of the wire as well as of the mesostresses acting on the scale of the individual crystallites [12]. In assumption of the anisotropic model and in using a finite-element method simulation, He et al. [11]calculated axial residual stress in cold drawn steel wires and obtained a good agreement with the X-ray diffraction measured results.

The main purpose of this study is to characterise some microstructural modification associated with additional torsion deformation of drawn wires. The cementite dissolution induced by additional torsion deformation has never been investigated in cold-drawn pearlitic steel wires before. It is the reason, while the aim of this investigation is to prove and discuss the cementite decomposition induced by torsion deformation of cold-drawn pearlitic steel wires and to propose an explanation to this cementite decomposition. Phase determination, quantification and carbon content variation in both phases is investigated by Mössbauer spectroscopy. This technique is very interesting to perform iron-based phase quantification and is very helpful to discriminate carbon repartition in samples and to quantify carbon concentration in individual phases. In the past, many studies of drawn pearlitic steel wires were performed in which different cementite dissolution mechanisms were proposed [1, 2, 4, 5, 7, 14–16]. Both mechanisms will be recalled in discussion. The comparison with Mössbauer phase quantification and carbon content determination would indicate their most probable occurrence induced by torsion deformation of initial cold-drawn eutectoid pearlitic steel wires.

Experimental procedure

The chemical composition of eutectoid pearlitic steel used in this investigation is listed in Table 1. Other elements such as Cu, Ni, Cr, Mo, P and S, are observed as trace (some ppm). Both wires were submitted to a cold drawing strain of $\varepsilon = 1.8$ which is the state of the reference sample. The size diameters of steel wires after drawing were 1.2 mm. During drawing, lubricant allows a warm elimination and the increase of temperature of draw dies as the system stays negligible. The steel wires average temperature was checked during deformation by means of an infrared camera (IR SnapShot 525). After drawing, using a free end torsion machine, the second specimen was submitted to a torsion deformation of $\gamma = 0.8$ in the first direction which was followed by a torsion deformation of $\gamma = 1.2$ in the reverse direction. The twist frequency is 2 Hz.

The nature and the microstructure of drawn pearlitic steel wires were characterised by Scanning Electron Microscopy, X-ray diffractometry and Mössbauer spectroscopy. Scanning electron microscopy (SEM) microstructural observations were performed on a 6500F JEOL FEG-SEM.

Specimens analysed by Mössbauer spectroscopy and X-ray diffraction are prepared as following. The drawn steel wires were cut in transverse axis to obtain from 30 to 50 of small pieces with the same length. The wire pieces were tied up in a compact faggot, which is embedded in a cold temperature epoxy matrix. Both planar faces of the as-cast specimen were mechanically polished with diamond paste up to 1 μm and then one of face was coated with conductive carbon film to make specimen conductor and avoid charge accumulation in the CXMS counter.

Mössbauer spectra was recorded at room temperature, in the conventional constant-acceleration mode, with a ^{57}Co(Rh) source, using a gas flow proportional counters. In Conversion X emission Mössbauer Spectroscopy (CXMS), the gas mixture in the counter is 5 vol.% CH_4/Ar. Mössbauer information come at $90 \pm 5\%$ from layers extending 2 μm, respectively, below the surface of the specimens [17]. The experimental Mössbauer spectra were analysed using a least square computer fit assuming

Table 1 Steel composition (in weight percent) of drawn wires

Chemical element	C	Mn	Si	Fe
Concentration (wt.%)	0.77	0.91	0.24	Balance

Lorentzian peak shapes, α-Fe as reference [18] and Mössbauer hyperfine parameters, characteristic of each iron environment were obtained. X-ray diffraction measurements were carried out with a Philips-Panalytical X'Pert Pro diffractometer, using a cobalt tube ($\lambda_{CoK_\alpha} = 0,1789$ nm), ($\lambda_{CoK_\beta} = 0,162$ nm) operating at 40 kV and 20 mA, and in a conventional goniometer mode (θ–2θ).

Results

Mössbauer spectra shown in Fig. 1 were recorded, at room temperature, in CXMS mode, on drawn wires specimen in as received state (reference) (a) and with additional mechanical deformation in torsion (b). Both specimen microstructures are ferrite and cementite with perhaps a very low amount of austenite (<0.9%) but this value is close to the limit of detection to be considered as been exact. Both spectra were separated in sextets and a single peak from which hyperfine parameters of each iron environment were determined by comparison with iron reference. These hyperfine parameters, summarised in Table 2, are the signature of iron without carbon in first neighbour position (noted O), iron with one or two carbon in first neighbourhood (noted I or II, respectively) in ferrite and cementite phases (noted α and Fe_3C, respectively). The cementite and ferrite quantifications with the carbon concentration determination in both phases were obtained and presented in Table 3.

According to the binary Fe–Fe_3C phase diagram, a carbon concentration in the range 0.8–0.9 wt.% C, after slow cooling, gives rise to a lamellae pearlitic structure corresponding to alternate lamellae of cementite and ferrite.[1] Then, the relative amount of cementite is in the range 0.8–0.9 wt.% C, which can be resumed, in theory, by a mean value of 12.75 ± 0.75%. As shown in Table 3, the cementite amount is always smaller than the theoretical value: with 8.5% in as-drawn wires and 4.8% after torsion deformation. In the same time, the carbon concentration in ferrite increases from 2.28 to 3.29 at.%. From the phase quantification and the carbon determination in individual phases, performed from Mössbauer measurements, it has been checked that the carbon content says content in specimen, even if locally this carbon concentration is changing by torsion deformation. Whenever the mechanical deformation state of wires, Mössbauer analysis gives rise to a global carbon content of 0.9 wt.% C, which is closed to the nominal value of pearlitic steel (0.8 wt.% C).

Phase characterisation performed by X-Ray diffraction is shown in Fig. 2. The microstructure of wires in as-received state (reference—drawn wires) (Fig. 2a) is

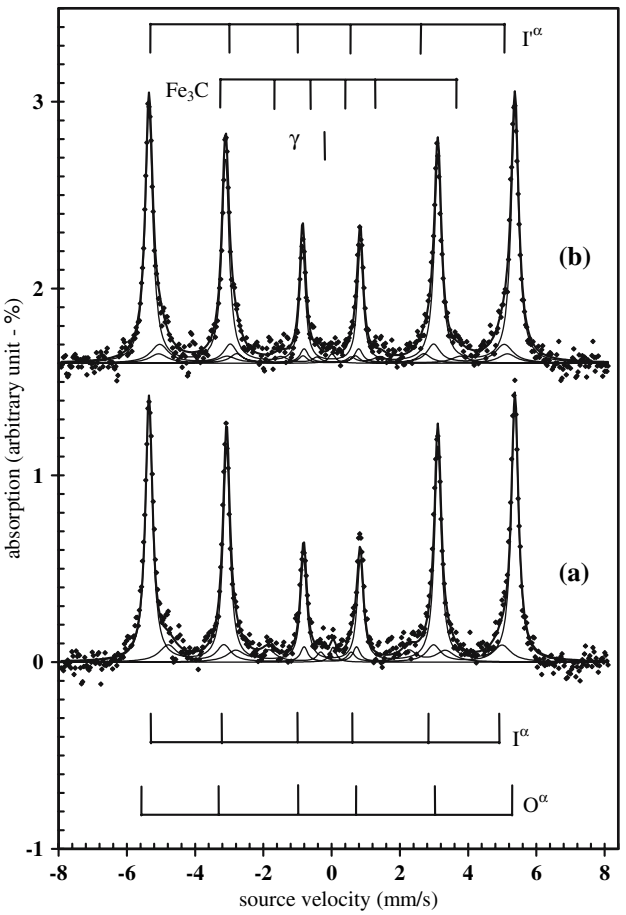

Fig. 1 Mössbauer spectra, recorded at room temperature in CXMS mode, on drawn wires specimen in as received state (reference) (**a**) and with additional mechanical deformation in torsion (**b**). The Co57 source velocity is in the range 8 mm/s–8 mm/s allowing simultaneous detection of magnetic and non-magnetic iron environments

characterised by ferrite and cementite diffraction peaks (the first peak located at 47° (2θ) corresponds to the K_β (110) peak). The crystallographic texture of the drawn pearlitic steel wires exhibit a strong [110] fibre along the axis of the wire induced by the drawing process [13]. After deformation, the texture evolves to a limit fibre texture [13]. This leads according to the used X-Ray experimental setup to some decrease of (110)α peak intensity compared to the (200) α and (211) α peaks intensities. The comparison between Fig. 2a and b shows diffraction peaks of ferrite, which are a little shifted to the left side after torsion deformation. This shift corresponds to an increase of lattice parameter, which could be attributed to the residual stresses introduced during the drawing and torsion processes or to an increase with the amount of interstitial carbon atoms in the bcc structure. Furthermore, the increase in carbon content in ferrite is checked by Mössbauer spectroscopy with average carbon content from 2 at.% to 3 at.%. The decrease or disappearance of Fe_3C diffraction peaks

[1] Fe-Fe3C phase diagram.

Table 2 Mössbauer hyperfine parameters of iron environments in drawn steel wires

	Site	H (kGauss)	IS (mm/s)	QS (mm/s)	W (mm/s)	A %	% phase	
Reference	0^{α}	333.9 ± 0.1	0.013 ± 0.1	−0,004 ± 0.1	0.24 ± 0.02	78.6 ± 3	αFe-C	91.4 ± 3
	$(I + I')^{\alpha}$	304.6 ± 0.1	0.009 ± 0.1	0.094 ± 0.1	0.56 ± 0.04	12.8 ± 2		
	II^{Fe3C}	191.4 ± 0.1	0.237 ± 0.1	0.024 ± 0.1	0.56 ± 0.04	8.6 ± 1.5	Fe_3C	8.6 ± 1.5
Torsion Deformation	0^{α}	333.9 ± 0.1	0.005 ± 0.1	0.004 ± 0.1	0.26 ± 0.02	75.8 ± 5	αFe-C	95.2 ± 4
	I^{α}	314.4 ± 0.1	0.010 ± 0.1	0 ± 0.1	0.55 ± 0.04	12.9 ± 3		
	I'^{α}	318.3 ± 0.1	0.002 ± 0.1	0.039 ± 0.1	0.55 ± 0.04	6.5 ± 2		
	II^{Fe3C}	212.8 ± 0.1	0.158 ± 0.1	0.196 ± 0.1	0.56 ± 0.04	4.8 ± 1.5	Fe_3C	4.8 ± 1.5

Table 3 Iron phase quantification and determination of carbon concentration performed from Mössbauer investigation

Phases	As received wires—Reference		Wires deformed in torsion	
	Phase amount (%)	Carbon concentration (at.%)	Phase amount (%)	Carbon concentration (at.%)
αFe-C (ferrite)	91.4 ± 3	2.28 ± 0.2	95.2 ± 4	3.29 ± 0.2
Fe_3C	8.6 ± 1.5	25	4.8 ± 1.5	25
Total carbon amount	0.9 ± 0.3 in wt.%		0.95 ± 0.3 in wt.%	

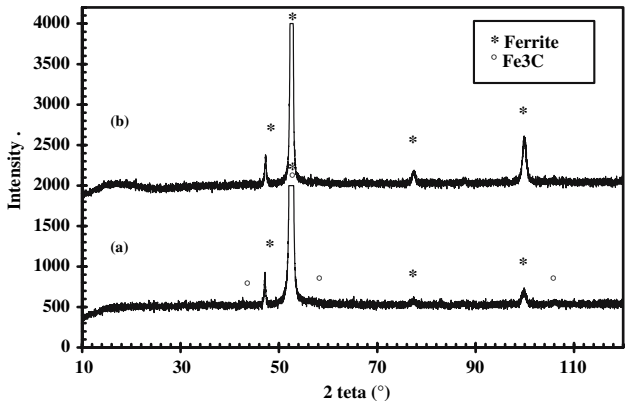

Fig. 2 X ray diffraction spectra, recorded at room temperature with a X Pert Pro diffractometer and Co tube ($\lambda_{K\alpha} = 1.790$ Å et $\lambda_{K\beta} = 1.62$ Å) on drawn wires specimen in as received state (reference) (**a**) and with additional mechanical deformation in torsion (**b**)

(Fig. 2b) after the torsion can be explained by different ways: dissolution or reorientation of the cementite, or fragmentation of the cementite associated to a large broadening of the peaks. The Fig. 3a shows the familiar microstructure obtained in drawn pearlitic wires observed by SEM: the lamellar structure forms lines oriented in the drawn direction. The Fig. 3b presents the same area of the wire after a direct and inverse torsion. We can observe a swirled and curled microstructure associated to large deformation of the microstructure.

As-observed during experiment, deformation in torsion in the opposite direction gives rise to a increase of the surface temperature up to a value estimated by Infra-red Camera to 90 °C. This temperature can be seen as a mean temperature, locally higher temperature will be expected.

Discussion

The initial chemical composition of wires, summarised in Table 1, shows a low amount of alloying element (0.91 wt.% Mn, 0.24 wt.% Si) with 0.8 wt.% of carbon atoms. So the influence of alloying element will be only limited to carbon atoms. Then, in the discussion, only the influence of carbon element, deformation strain and cooling rate will be responsible of the initial lamellar microstructure of steel and of its evolution with the drawing process.

From Mössbauer spectroscopy and X-ray diffraction measurements, a microstructure comparison of the drawn pearlitic steel with lamellae structure of pearlitic steel is allowed. Then, by those techniques, it was found that drawing is responsible of:

- A lower amount of cementite (8.5%) than in pearlitic steel at the same chemical composition (12.75%);
- A higher level of carbon concentration in bcc ferrite, 2.3 at.%, compared to the 0.1 at.% as shown in binary phase diagram steel (see footnote 1);
- Diffraction peak broadening, which is the sign of the nanostructured phase, internal stress or disordered structure.

Even if the mechanical properties investigation is not the purpose of this study, as reported in the literature [14, 16], mechanical properties and microstructure modifications are intimately acquainted and the drawing process modifies the mechanical properties of drawn pearlitic steel wires with the deformation increase. The evolution of tensile strength, work hardening rate and ductility, during

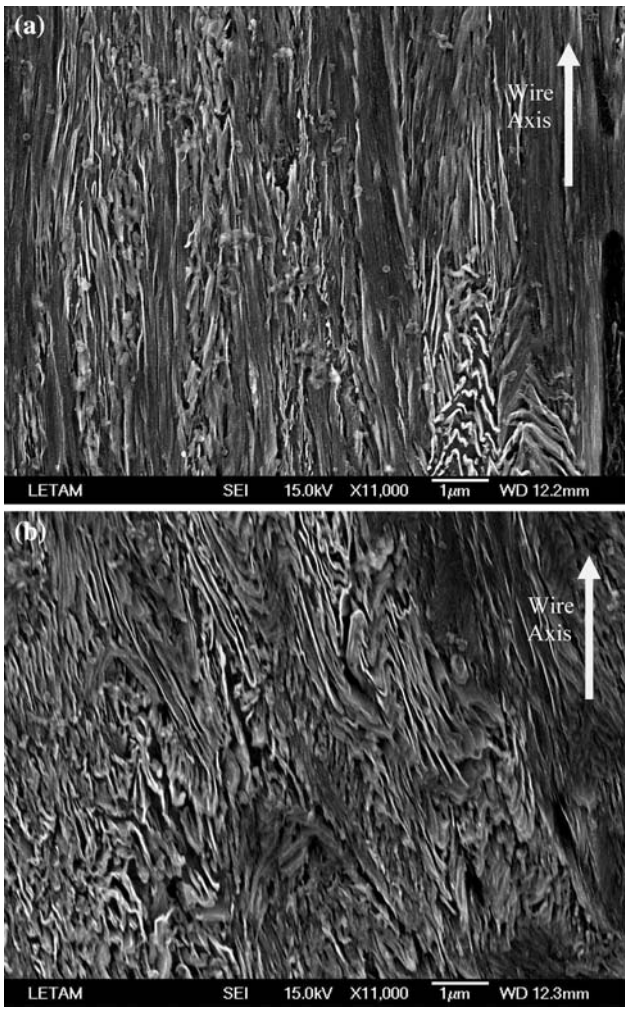

Fig. 3 SEM observation of the near-surface of wires in a plane including the wire axis (**a**) As received drawn wire (**b**) Microstructure of wires submitted to a direct and reverse torsion

wire drawing, separately depend on refinement of interlamellae spacing, and on nature of alloying elements [19].

The dissolution of cementite associated with a high carbon amount in ferrite, detected by Mössbauer spectroscopy, is in good agreement with literature [1, 2, 4, 5, 7, 14, 16, 19]. The mechanisms of cementite decomposition, carbon atoms migration and enrichment in carbon of ferrite, which are considered in literature [1, 2, 15, 19], are associated to a significant dislocations role. Now, in the following sentence, both of them are summarized. P. Watté et al. [15], have proposed a mechanism decomposed in two different stages and have schematised its beneficial opportunity in the representation of the energy diagram [15] (Fig. 4). In the first stage, in moving in ferrite phase, dislocations pin carbon in interstitial sites of the b.c.c. structure. This induces a decrease of the dislocation mobility but it is not enough to stop them and ferrite becomes heterogeneous in carbon composition, its ductility decreases and hardness increases [15]. In the second stage, dislocations pump carbon atoms and then transfer carbon element from cementite to ferrite inducing cementite decomposition [15]. The ferrite dislocations pinning by carbon atoms increases, locking the ferrite dislocations which can be mechanically depicted by an additional hardness increase and chemically by a carbon sursaturation in ferritic phase.

As a consensus, Gavriljuk and many other authors [1, 2] explain cementite decomposition in pearlitic steel and resulting dissolution of carbon in ferrite, in term of higher enthalpy of binding between carbon atoms and dislocations in ferrite than in cementite. It would be the reason while the cementite decomposition is controlled by the transfer of carbon atoms from cementite to dislocations accumulated near the interface during deformation. Furthermore, in pearlitic steel, this binding enthalpy between carbon atoms and dislocations in ferrite is influence by alloying elements and the interatomic bonds in cementite affect the stability of cementite under cold work. The binding energy affects the hardness of cementite and its ability to deform rather than to dissolve [1]. The fraction of the cementite decomposed increases with the increase of the interfacial area between ferrite and cementite and the decomposition becomes less intensive at higher strains.

Cementite dissolution and a large number of defects were reported, too, by Languillaume et al. [7], after cold drawing of pearlitic steel wires (0.7 wt.% C). Both the cementite dissolution and the large number of defects, which are manifest as a high density of interfaces, due to the strong microstructural refinement (interlamellae spacing close to 20 nm containing high internal elastic strains) occurring during wire drawing [7]. The interpretation of Languillaume et al. [7] is based on cementite dissolution due to phase destabilisation by increase of its free energy arising from thinning of cementite lamellae and creation of slip steps during wire drawing. A high level of microstrain is present in the microstructure and is thought to result from a metastable state of the interfaces due to dislocation incorporation. This interpretation is an alternative to the interpretation found in the literature based on carbon-dislocation interactions and could be applied to the present study. Hence, the free energy of the cementite is increased by an interfacial contribution to such an extent that cementite becomes unstable and dissolves into a supersaturated solid solution of carbon in ferrite. From Mössbauer and X-ray diffraction measurements, it is impossible to determine the best mechanism of cementite dissolution and carbon enrichment of ferrite, depicting the microstructure evolution under drawing. Further analysis of dislocations repartition by transmission electron microscope will be needed.

The relative peaks intensities and the broadening of diffraction peaks are in good agreement with a

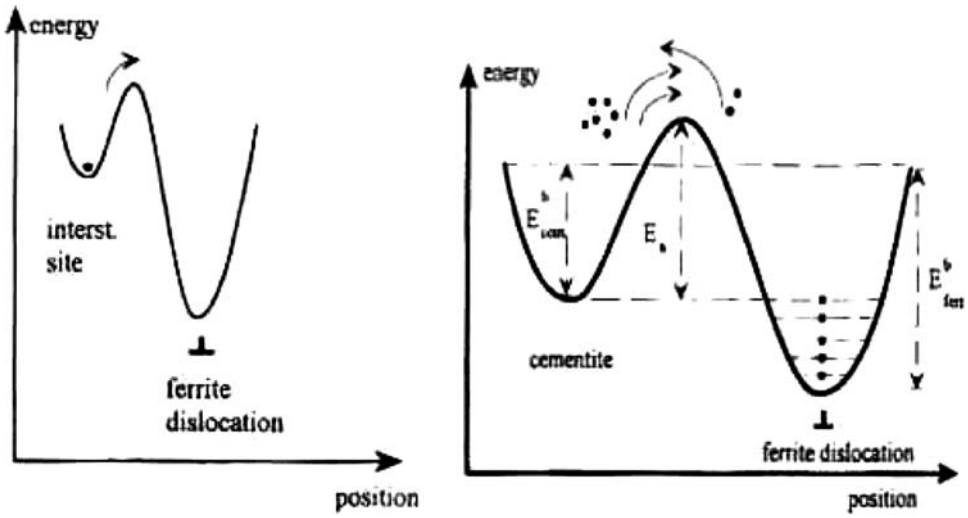

Fig. 4 Strain ageing of heavily drawn pearlitic steel wires: Schematic representation of an energy diagram which explains the transfer of carbon atoms from an interstitial site to a dislocation during first stage (**a**) and the transfer from cementite to ferrite dislocations during the decomposition of cementite during the second stage of strain ageing (**b**) [15]

fragmentation of cementite lamellae, thinner deformed ferrite lamellae, and nanocrystalline phase reported by different authors [4, 7, 14, 16]. The high tensile stress in alternated cementite and ferrite lamellae, induced by cold-drawn to $\varepsilon = 1.8$, is responsible of X-Ray peaks broadening [10]. Cementite lamellae are subject to a high tensile stress and ferrite lamellae to compressive stress [10].

In fact, in these studies, drawing was reported to induce co-deformation of ferrite and cementite phases, and cementite fragmentation into planar nanoscale particles [14, 16].

During the torsion deformation the temperature is increased. As shown by the microstructural investigation (Table 3, Figs. 1 and 2), after torsion deformation, wires are characterised by a lower amount in cementite (cementite quantification of 4.8% in Mossbauer spectroscopy), a carbon enrichment of ferrite phase (3.3 at.% C compared to 2.3 at.% before), a lower texture in ferrite phase and thicker diffraction peaks compared to as-drawn material as shown in Fig. 2b. Both modifications are the result of individual or conjugal temperature increase and torsion deformation effects.

It is known that the temperature elevation favours carbon diffusion in ferrite, cementite and at the interface between both phases. Stress relaxation is also expected but for higher temperature [10, 20, 21]. As shown by Mössbauer spectroscopy and XRD diffractograms, the cementite is not regenerated because its amount evolutes in opposition with smaller values after the wires torsion. The lower cementite amount is attributed to the effect of torsion deformation and temperature increase.

Earlier, unidirectional and reverse torsion test were performed on wires by Goes et al. [16]. Fracturation after torsion is a complex event dependent on the shear stress and strain at the primary fracture moment, the surface density and size distribution of the microcracks in the wire, and the samples length. Most frequently, in the first step of torsion deformation test, as a result the high level of elastic energy stored in the wires, multiple fragmentations of the samples are observed [16]. The secondary fractures, which appear after, are the consequence of the meeting of pre-existing surface micro-defects [16]. Hence, the lower cementite concentration, observed by CXMS and XRD analysis, could be explained by fragmentation of cementite crystallites during torsion test, increase of defects such as microcracks and dislocations. Carbon could be transferred from cementite to ferrite by dislocation. Any way, in our investigation, micro or macrocracking has not been detected by any microscopic techniques. In the torsion deformation applied to as-drawn wires, the level of shear stress and strain are too small to provide some cracking or fractures. This result seems not to be really in agreement with Goes study [16]. In fact, the level of torsion deformation applied is smaller than the one used in Goes's investigation and we do not have to forget the influence of the increase of temperature, observed during wires torsion, on microstructural modification and on rearrangement of dislocations and interstitials defects.

The plastic deformation during the torsion of steel wires can usually be regarded as a simple shear deformation with a shear plane perpendicular to the wire axis and a shear direction tangent to the wire surface. Since the strain when the wire passes through the die is of a more complex nature including shear and compression strain, the deformation involved in torsion is highly different. The deformation of the crystalline material, under applied load, is only possible if dislocations are able to move across the material. During the slip and climb of dislocations, cementite is fragmented. Successively, free carbon atoms are released in the solid solution. These interstitial atoms act as impurities and pin up the dislocations. The distance between cementite lamellas mainly determines the strength of the cold-drawn

pearlitic steel wire. Pinning of dislocations by carbon atoms affects ductility. The material reacts in order to release local internal stresses and to allow a higher deformation without breaking. Hence, locally, the lattice friction is responsible of an increase of temperature, which assists the dislocation in their trips. Then, dislocations are not blocked in cementite or ferrite phases or at the interface of both phases (phase or grain boundaries). At this temperature, the dislocations are, again, able to tract carbon atoms along their driving and further deformation of steel wire in torsion is able to be performed. Carbon atoms which move with mobile dislocations are accumulated in ferrite phase which becomes super-sursaturated as confirmed by the value of 3.3 at.% C measured in ferrite by Mössbauer spectroscopy

The increase of temperature, corresponding to a mean temperature with certainly more higher local temperature, allows possible cementite recombination. The final amount of cementite (4.8%) cannot be seen as negligible: the level of successive tensile and torsion deformations is not enough to be responsible of complete cementite decomposition as referred in literature [4, 5, 7]. The increase in cementite dissolution is certainly associated to the new dislocation structure induced by torsion, which offers new possibilities for taking out the carbon from cementite.

Conclusion

Pearlitic steel wires in as-drawn state ($\varepsilon = 1.8$) and after additional torsion ($\gamma = 0.8$ following by $\gamma = 1.2$ in reverse direction) have been studies by Mössbauer spectroscopy, X-Ray diffraction and Scanning Electron Microscopy. Alloying elements such as are in small amount in the pearlitic steel and will not significantly influence morphology and composition of the pearlitic microstructure or the displacement speed of dislocations.

The microstructure evolves with the level and the nature of the deformation. The observed increase of temperature assists the wire deformation. By comparison with equilibrium Fe–Fe_3C binary phase diagram, due to drawing process, the amount of cementite, in as-drawn wires, is smaller and the carbon concentration in ferrite is much higher (>0.1 at.%). The torsion deformation induces an increase of carbon atom concentration in ferrite associated to a decreased cementite amount compared to as-drawn wires, nevertheless, without total disappearing of cementite phase.

The mechanisms of deformation, by drawing, are known to be the results of cementite fragmentation and dissolution and to induce an increase of defects such as dislocations. The mobility of dislocation in the first stage of deformation by drawing helps carbon atoms diffusion. In a second stage, these dislocations are pinned by interstitial carbon atoms (release by cementite dissolution) and blocked in ferrite near the interface between the lamellae or grains. The result is the sursaturation in carbon atoms of the ferrite lattice.

During torsion deformation, the mechanisms of deformation, which regulate steel microstructure are attributed to the evolution of density and nature of defects (dislocation or free atoms), to lattice friction and to ability of the lattice to reduce the internal stress create by application of external stress and by interactions toward defects. As the wires are deformed in torsion, shear stress and the associated shear strain induce lattice friction. This friction is responsible of the global and local temperature increases and helps the material to over-deform. Then, the carbon atoms diffusion by dislocation moving is possible and high enough to allow wires deformation without cracking or breaking.

In the future, the material, in which wires were fabricated, presents a high ability to be deformed in torsion and wires must not be cooled, during torsion deformation, if we want to avoid any break of them.

Acknowledgement The authors acknowledge one of the referees for valuable comments.

References

1. Gavriljuk V (2002) Scripta Materialia 46(2):175
2. Gavriljuk VG (2003) Mater Sci Eng A 345(1–2):81
3. Maruyama N, Tarui T, Tashiro H (2002) Scripta Materialia 46(8):599
4. Shabashov VA, Korshunov LG, Mukoseev AG, Sagaradze VV, Makarov AV, Pilyugin VP, Novikov SI, Vildanova NF (2003) Mater Sci Eng A 346(1–2):196
5. Embury JD, Fisher RM (1966) Acta Metall 14(2):147
6. Makii K, Yagushi H, Ibaraki N, Miyamoto Y, Oki Y (1997) Scripta Materialia 37:1753
7. Languillaume J, Kapelski G, Baudelet B (1997) Acta Materialia 45(3):1201
8. Tomota Y, Suzuki T, Kanie A, Shiota Y, Uno M, Moriai A, Minakawa N, Morii Y (2005) Acta Materialia 53(2):463
9. Tomota Y, Luká P, Neov D, Harjo S, Abe YR (2003) Acta Materialia 51(3):805
10. Van Acker K, Root J, Van Houtte P, Aernoudt E (1996) Acta Materialia 44(10):4039
11. He S, Van Bael A, Li SY, Van Houtte P, Mei F, Sarban A (2003) Mater Sci Eng A 346(1–2):101
12. Yu Zolotorevsky N, Yu Krivonosova N (1996) Mater Sci Eng A 205(1–2):239
13. Liu Y, Jiang QW, Wang G, Wang YD, Tidu A, Zuo L (2005) J Mater Sci Technol 21(3):357
14. Hono K, Ohnuma M, Murayama M, Nishida S, Yoshie A, Takahashi T (2001) Scripta Materialia 44(6):977
15. Watté P, Van Humbeeck J, Aernoudt E, Lefever I (1996) Scripta Materialia 34(1):89
16. Goes B, Martín-Meizoso A, Gil-Sevillano J, Lefever I, Aernoudt E (1998) Eng Frac Mech 60(3):255

17. Cordier-Robert C, Foct J, Iost A (2000) In: Sudarshan TS, Jeandin M (eds) Proceedings of the fourteen international conference on surface modification technologies, Paris (France). ASM International, USA, p 345
18. Le Caër G, Thèse d'Etat, Ecole des Mines de Nancy (1974)
19. Song HR, Kang EG, Nam WJ (2007) Mater Sci Eng A 449–451:1147
20. Zeren A, Zeren M (2003) J Mater Process Technol 141(1):86
21. Read HG (1997) Scripta Materialia 37(2):151